Three dimensional imaging of ventilation dynamics in obstructive lung disease

J. H. Holmes[1], R. L. O'Halloran[1], E. K. Brodsky[1,2], T. A. Bley[2], C. J. Francois[2], J. V. Velikina[1], R. L. Sorkness[3], W. W. Busse[3], and S. B. Fain[1,2]

[1]Department of Medical Physics, University of Wisconsin-Madison, Madison, WI, United States, [2]Department of Radiology, University of Wisconsin-Madison, Madison, WI, United States, [3]Department of Medicine, University of Wisconsin-Madison, Madison, WI, United States

Introduction: The technique described in this work demonstrates the first true 3D time-resolved lung imaging technique enabling the acquisition of a wealth of information on inflow and exhalation kinetics as well as breath-held ventilation defects within a single comprehensive maneuver. This is all done while readily accommodating individual patients' breath-hold capabilities. Rapid 2D and multi-slice imaging methods have been used for depicting time-resolved regional heterogeneity of obstructive lung disease using hyperpolarized He-3 (HPHe3) gas [1,2,3]. A multi-echo projection acquisition (ME-VIPR) has been shown for 3D imaging of respiratory dynamics as well as to accommodate variable patient exhalation and inhalation times [4]. The HighlY constrained back PRojection algorithm has been demonstrated for decreasing undersampling artifact and improving SNR for depicting contrast kinetics [5] and the modified iterative approach (I-HYPR) [6] has been demonstrated for dynamic imaging of nonsparse datasets. Although the rapid 2D, multi-slice, and 3D VIPR techniques provide improvements over conventional methods, there is still a need to improve SNR of 3D time-resolved HPHe3 images. The work presented here makes use of the ME-VIPR acquisition to improve data collection efficiency and the I-HYPR reconstruction to improve SNR to enable 3D time-resolved imaging of HPHe3 respiratory dynamics with whole-lung coverage.

Methods: Ten volunteers (8 asthmatics, 1 pulmonary aneurysm, 1 normal) underwent dynamic HPHe3 MRI and MDCT (multi-detector CT) for analysis of gas trapping. MRI studies were performed on a 1.5 T clinical scanner (Signa HDx, GE HealthCare, Milwaukee, WI). A fully 3D ME-VIPR 8-halfecho k-space trajectory was acquired, with a modification to the angular sampling such that 3 of the angles were full projections spanning the full diameter of k-space to better accommodate the geometric assumptions required by the I-HYPR reconstruction. Unique interleaved angle sets were acquired every 0.1 s, each set covering the full sphere of k-space. This sampling ordering allowed cine-type reconstruction to accommodate variable patient breath-hold times. I-HYPR images were reconstructed with of 1 s of time-frame data and 6 iterations. HPHe-3 gas was prepared to a polarization level of ~28% using a commercial polarizer (GE Healthcare, Waukesha, WI). The HPHe3 gas was then mixed with nitrogen to produce a dose of ~4.5 mM polarized nuclei for an inhaled volume of 14% of the volunteer's total lung capacity (TLC) from functional reserve capacity (FRC). Dynamic HPHe-3 MRI was performed during a single patient respiration maneuver including inspiration, breath-hold, forced expiration, and followed by tidal breathing for a total time of 40-60 s. MDCT images were acquired during two separate breath-holds of 4-6 s at TLC and FRC to depict airway structure and regions of potential gas trapping (GE LightSpeed, GE Healthcare, Waukesha, WI). Two radiologists evaluated the MR data for evidence of gas trapping by consensus and blinded to MDCT data. Following this, MDCT data was also read by consensus. RV (residual volume) and TLC were measured with the volunteer in a relatively passive state and the subsequently derived measure of gas trapping RV/TLC is designated slowRV/TLC for this work. Dynamic air trapping was designated fastRV/TLC where fastRV is the difference between TLC and FVC (forced vital capacity) [7].

Results: A subset of maximum intensity projection (MIP) images from a dynamic ventilation study are shown in a volunteer with a pulmonary aneurysm displaying abnormalities visible during inspiration and gas trapping during expiration (Fig. 1a arrows). The uptake slope map for the pulmonary aneurysm case shows elevated uptake in the parenchymal region adjacent to the region of gas trapping (Fig. 1b arrow). The diagnosis of gas trapping was established using MDCT in 6 of the 10 patients. Gas trapping was detected in 5 of these same 6 volunteers using MRI, with significant trapping found in 2 volunteers (1 asthmatic and 1 pulmonary aneurysm). MRI and MDCT results are shown for an asthmatic depicting regions of ventilation defects on MRI during breath-hold (Fig. 2a arrows), regions of gas trapping during forced expiration (Fig. 2b arrows), and confirmation of gas trapping detected on MDCT comparing breath-holds at TLC (Fig. 2c) and FVC (Fig. 2d arrows). Of the 5 volunteers that displayed gas trapping on both MRI and MDCT, 47 % of the gas trapping locations were detected using both modalities. The regions in disagreement were small to moderate regions of air trapping on MDCT or MRI (size of trapped regions < 4 cm). However, only 1 volunteer was found to exhibit small regions of gas trapping on MDCT that were not detected using MRI (size of trapped regions ≤ 1 cm). Focal regions of abnormally rapid gas uptake were observed during inhalation in 5 of the volunteers on MRI. The mean values of fastRV/TLC were found to be significantly different for volunteers displaying gas trapping on MRI from those showing no trapping ($p = 0.05$), however the means were not significant for FEV1%pred ($p = 0.16$) or slowRV/TLC ($p = 0.27$). To focus on asthma, the volunteer diagnosed with a pulmonary aneurysm (having severe gas trapping) was not included for this analysis.

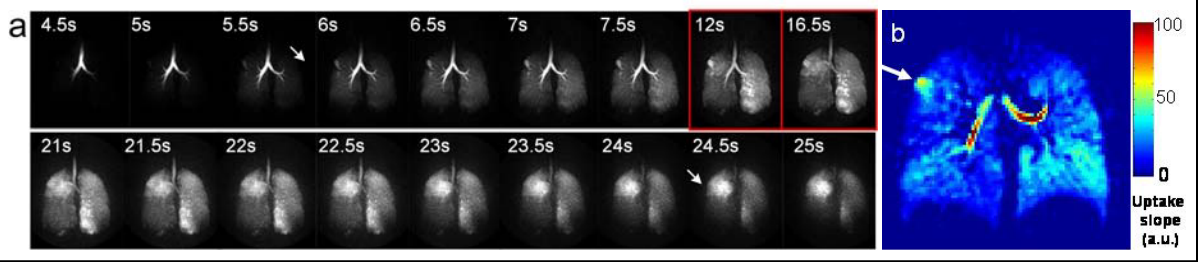

Figure 1. Subset of MIP time-frame images during dynamic ventilation showing intense signal enhancement during inspiration (arrow, 6 s) and significant trapping in the upper right lobe in a volunteer with a pulmonary aneurysm (arrow, 24.5 s). a) Uptake slope map depicting region of abnormal gas uptake during inspiration in same volunteer as a) (arrows).

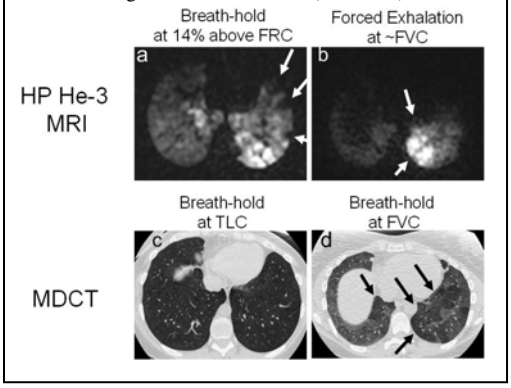

Figure 2. HP He-3 MRI with MDCT showing ventilation defects during the breath-hold (a, white arrows) in a volunteer with asthma. During the forced exhalation, residual signal due to gas trapping is evident in MRI (b, arrows) and air trapping is confirmed in MDCT during breath-hold at FRC (d, arrows).

Conclusions: Whole lung 3D imaging of respiration dynamics has been demonstrated in asthmatics and normals, and detection of gas trapping has been compared with MDCT and spirometry. This 3D technique provides the ability to detect regional dynamic airway closer and differences in signal kinetics at high spatial and temporal resolution. Note that while CT can provide static information about regional gas trapping, it is unable to depict dynamic closure in a setting more comparable to a spirometry maneuver. Future work will include applying these methods to the study of childhood asthma and determining gas trapping reproducibility as well as guided interventions based on segmentation of the airway tree [8] and bronchoscopic assessment.

References: [1] Salerno et al. MRM 2001;46:667-677 [2] Koumellis et al. JMRI 2005;22:420-426 [3] Holmes et al. JMRI 2007;26:630-636 [4] Holmes et al. MRM 2008;59:1062-1071[5] Mistretta et al. MRM 2006;55:30-40 [6] O'Halloran et al. MRM 2008;59:132-139461 [7] Wenzel et al. Am J Crit Care Med 1999;160:1001-1008 [8] Peterson et al. ISMRM 2008 abstract 2645